

# Partial dysferlin reconstitution by adult murine mesoangioblasts is sufficient for full functional recovery in a murine model of dysferlinopathy

J Díaz-Manera<sup>1,2,3</sup>, T Touvier<sup>1</sup>, A Dellavalle<sup>1</sup>, R Tonlorenzi<sup>1</sup>, FS Tedesco<sup>1</sup>, G Messina<sup>1,4</sup>, M Meregalli<sup>5</sup>, C Navarro<sup>5</sup>, L Perani<sup>1</sup>, C Bonfanti<sup>1</sup>, I Illa<sup>2,3</sup>, Y Torrente<sup>5</sup> and G Cossu<sup>\*,1,4</sup>

Dysferlin deficiency leads to a peculiar form of muscular dystrophy due to a defect in sarcolemma repair and currently lacks a therapy. We developed a cell therapy protocol with wild-type adult murine mesoangioblasts. These cells differentiate with high efficiency into skeletal muscle *in vitro* but differ from satellite cells because they do not express Pax7. After intramuscular or intra-arterial administration to *SCID/BLAJ* mice, a novel model of dysferlinopathy, wild-type mesoangioblasts efficiently colonized dystrophic muscles and partially restored dysferlin expression. Nevertheless, functional assays performed on isolated single fibers from transplanted muscles showed a normal repairing ability of the membrane after laser-induced lesions; this result, which reflects gene correction of an enzymatic rather than a structural deficit, suggests that this myopathy may be easier to treat with cell or gene therapy than other forms of muscular dystrophies.

*Cell Death and Disease* (2010) 1, e61; doi:10.1038/cddis.2010.35; published online 5 August 2010

**Subject Category:** Neuroscience

Mutations in the human dysferlin gene (*DYSF*) cause an autosomal recessive muscular dystrophy with different clinical phenotypes: limb girdle muscular dystrophy (LGMD-2B), distal posterior myopathy or Miyoshi's myopathy, distal anterior myopathy, asymptomatic hyperckemia and the recently described, congenital muscular dystrophy.<sup>1–3</sup> Generally, the first symptoms appear in the late teens or early in adulthood.<sup>4</sup> The rate of progression is variable, although the majority of patients develop a severe clinical situation characterized by inability to walk without support or confinement to a wheelchair within 10–20 years from the onset of symptoms.<sup>5</sup>

Two different naturally occurring murine models with mutations in the dysferlin gene have been described: the *A/J* and *SJL* lines.<sup>6</sup> The genetic modification of the *A/J* strain consists in a unique ETn retrotransposon insertion near the 5' end (intron 4) of the dysferlin gene producing the complete loss of the protein.<sup>6</sup> *A/J* mice develop a late-onset and slowly progressive muscular disease. The first dystrophic features appear at 4–5 months, affecting both lumbar and proximal muscles of the lower limbs. By 9 months of age, dystrophic muscles present variation in fiber size, moderate fatty infiltration and sparse necrotic fibers surrounded by macrophages infiltrates.<sup>7</sup>

The function of dysferlin in skeletal muscle is related to membrane repair. It has been shown that dysferlin is required for the fusion of intracellular vesicles to the membrane and consequent resealing of the sarcolemma after external damage.<sup>8</sup> In support of this hypothesis, nonfused intracellular vesicles near the surface of the muscular fibers have been described in biopsies from affected patients.<sup>9</sup> Moreover, no recovery of sarcolemma integrity was observed after laser-induced lesions in the membrane of isolated single fibers from dysferlin-deficient mice.<sup>10,11</sup>

Mesoangioblasts (MABs) are vessel-associated progenitors<sup>12</sup> that can be isolated from different embryonic and adult tissues, expanded *in vitro*, easily transduced with lentiviral vectors and have the ability to cross the vessel wall when injected into the bloodstream.<sup>13</sup> Intra-arterial delivery of murine and canine MABs, respectively, ameliorated the dystrophic phenotype of *Sgca* null mice (a murine model of LGMD-2D) and of Golden Retriever dogs affected by a dystrophin deficit (a natural occurring model of Duchenne muscular dystrophy (DMD)).<sup>14,15</sup> Similar cells isolated from human postnatal skeletal muscle were shown to represent a subset of pericytes and were able to give rise to dystrophin-positive muscle fibers when transplanted into *scid/mdx* mice.<sup>16</sup> Based on these studies, a phase I clinical trial with

<sup>1</sup>Division of Regenerative Medicine, San Raffaele Scientific Institute, 58 via Olgettina, Milan 20132, Italy; <sup>2</sup>Neuromuscular Diseases Unit, Neurology Department, Hospital Santa Creu i Sant Pau, Universitat Autònoma de Barcelona, 167 Sant Antoni Maria Claret, Barcelona 08025, Spain; <sup>3</sup>Centro de Investigación Biomédica en Red sobre Enfermedades Neurodegenerativas, Madrid 28031, Spain; <sup>4</sup>Department of Biology, University of Milan, 26 via Celoria, Milano 20133, Italy and <sup>5</sup>Stem Cell Laboratory, Department of Neurological Sciences, Fondazione IRCCS Ospedale Maggiore Policlinico, Centro Dino Ferrari, Università di Milano, via F. Sforza 35, Milano 20122, Italy

\*Corresponding author: G Cossu, Division of Regenerative Medicine, San Raffaele Scientific Institute, 58 via Olgettina, Milan 20132, Italy.

Tel: +39 02 2643 4954; Fax: +39 02 2643 4621; E-mail: cossu.giulio@hsr.it

**Keywords:** mesoangioblasts; stem cells; dysferlin; therapy; *A/J* mice

**Abbreviations:** MABs, mesoangioblasts; DMD, Duchenne muscular dystrophy; PM, proliferation medium; DMEM, Dulbecco's modified Eagle's medium; IF, immunofluorescence; WB, western blot; MHC, myosin heavy chain; TGF- $\beta$ , transforming growth factor  $\beta$ ; BMP-2, bone morphogenic protein-2; AP, alkaline phosphatase

Received 14.4.10; revised 25.5.10; accepted 10.6.10; Edited by G Melino

MAB allo-transplantation in DMD patients is at this moment in the recruitment phase.

In this study, we isolated and characterized MABs from muscular biopsies of adult *C57BL/6* wild-type mice (C57-J1 cells). These cells shared several characteristics with previously described embryonic mouse MABs (e.g., the D16 cells), such as the ability to differentiate into other mesenchymal tissues or the capacity to cross the vessel wall and colonize dystrophic muscles after intra-arterial injection. However, at variance with D16 cells, and similar to human postnatal MABs, C57-J1 cells spontaneously differentiate into skeletal myotubes with high efficiency; yet they differ from *bona fide* satellite cells (SCs) for the absence of Pax7 expression. Here we show that after transplantation into the dysferlin-deficient murine model *SCID/BLAJ*, C57-J1 cells were able to fuse with muscle fibers, restoring the expression of dysferlin and causing normalization of the resealing capacity of the plasma membrane.

## Results

### Characterization of adult murine-derived MABs (C57-J1).

Adult-derived MABs were isolated from the tibialis anterior of a 2-month-old *C57BL/6* female mouse.<sup>17</sup> When cultured in proliferation medium (PM), they showed a small, refractile morphology and proliferated rapidly, with a doubling time of approximately 24 h (Figure 1a). During proliferation, virtually all cells expressed at high level the surface markers Sca-1 and CD44 (Supplementary Figure 1) but, in contrast to SCs, they did not express detectable levels of MyoD or Pax7 (Figure 1e and f). Unexpectedly, they did not express alkaline phosphatase (AP) (Supplementary Figure 2a) similar to their human counterparts.<sup>18</sup>

Once confluent, they progressively differentiated into striated muscle (Figure 1b). On average, 25–40% of cells fused into striated, myosin-positive, multinucleated myotubes (Figure 1c and d). Myogenic differentiation was not influenced by the substratum (Matrigel *versus* plastic; Supplementary Figure 2d). The myogenic transcription factors MyoD and Myogenin were robustly expressed only after 48 h in differentiation medium, at the onset of myotube formation, and underwent a progressive reduction in the expression level after day 4 (Figure 1e). The expression of dysferlin was clearly detectable in myotubes concomitant with MyoD expression (Figure 1e). Its concentration increased progressively peaking up at days 6 and 8, concomitant with the maximum fusion of mononucleated cells into myotubes (Figure 1c and e).

Despite their spontaneous myogenic differentiation potency, C57-J1 cells were also able to differentiate *in vitro* into other mesoderm tissues upon exposure to proper inductive signals, as previously described for other MAB lines. After treatment with bone morphogenic protein-2 (BMP-2), they expressed AP whereas they expressed smooth muscle actin when treated with transforming growth factor- $\beta$  (TGF- $\beta$ ); moreover, after 6 days of culture into adipogenic medium, rounded intracellular oil-red-positive vesicles were detected. (Supplementary Figures 2a–c).

**Engraftment failure in *A/J* mice and generation of *A/J SCID* strain.** To investigate the ability of adult-derived murine MABs to restore the expression of dysferlin in dystrophic

muscles, we injected  $5 \times 10^5$  C57-J1 cells, previously transduced with lentiviral vector expressing nuclear LacZ, into the tibialis anterior and quadriceps of 5-month-old *BLAJ* mice ( $n=7$ ) (generous gift from I Richard, Généthon). At 36 h after the injection, numerous nuclear LacZ (nLacZ)-positive cells were detected in the muscles, but they appeared already surrounded by an inflammatory infiltrate composed by neutrophils, CD68+ macrophages and CD3+ T lymphocytes (Figure 2a). The inflammatory infiltrate increased progressively until day 7, when numerous CD68+ cells were localized in the injection area, but also in distant areas of the muscle and in the vessel walls (data not shown). By day 12 we detected some degenerating muscle fibers with LacZ-positive nuclei surrounded by CD68+ and CD3+ cells (Figure 2b). At 3 weeks after the injection muscle regeneration was completed, probably at the expense of resident SCs because no LacZ-positive cells could be detected either inside or outside fibers, whereas some CD68 and CD3 cells remained in the perimysium (Figure 2a). This result may depend upon the altered immune response of *BLAJ* mice characterized by a more aggressive phagocytic activity of macrophages and a reduced expression of decay-accelerating factor (DAF) in muscles.<sup>19,20</sup> Because of these results, we decided to generate a dystrophic, immune-deficient mouse by crossing *BLAJ* mice onto an *SCID* mouse background (*SCID BLAJ*). The F4 generation used in this study showed absence of mature T and B lymphocytes by FACS analyses (data not shown) and the presence of retrotransposon insertion in dysferlin gene, as originally described in the *A/J* strain by Ho *et al.*<sup>6</sup> At 5 months of age, *A/J SCID* and *BLAJ* mice showed dystrophic changes, such as central nuclei, fiber splitting, variation on fiber size and presence of regenerating fibers (Supplementary Figure 3a). Azan Mallory staining showed a similar degree of fibrosis in both *AJ/SCID* and *BLAJ* model compared to the control (Supplementary Figure 3a). As expected, immunofluorescence (IF) analysis and reverse transcription (RT)-PCR staining confirmed the absence of dysferlin expression (Supplementary Figure 3b and c).

### Restoration of dysferlin expression by injection of C57-J1 cells into the new *SCID/BLAJ* line.

We tested the ability of C57-J1 cells to restore the expression of dysferlin in muscles from the *SCID/BLAJ* mice. We performed a single intramuscular injection of  $5 \times 10^5$  nLacZ labeled C57-J1 cells in untreated or cardiotoxin (ctx)-pretreated tibialis anterior, quadriceps and gastrocnemius of 5-month-old *SCID/BLAJ* mice ( $n=6$  mice, 3 pretreated with ctx). ctx was used to exacerbate the pathology of these mice that at 5 months show a less severe phenotype than other strains such as the  $\alpha$ -sarcoglycan null mice, previously used for MAB transplantation.<sup>13</sup> At 1 month after the injection, numerous nLacZ-positive fibers were detected in transverse muscle sections at different craniocaudal levels (Figure 3a); although nLacZ-positive fibers were diffuse in the ctx-treated muscles, they were more concentrated near the injection area in the untreated muscles. In parallel, we performed a single intra-arterial injection of  $5 \times 10^5$  nLacZ labeled C57-J1 cells into the right femoral artery of untreated and ctx-treated, 5-month-old *SCID/BLAJ* mice ( $n=10$ , 5 pretreated with ctx). To increase susceptibility of muscles to engraftment by

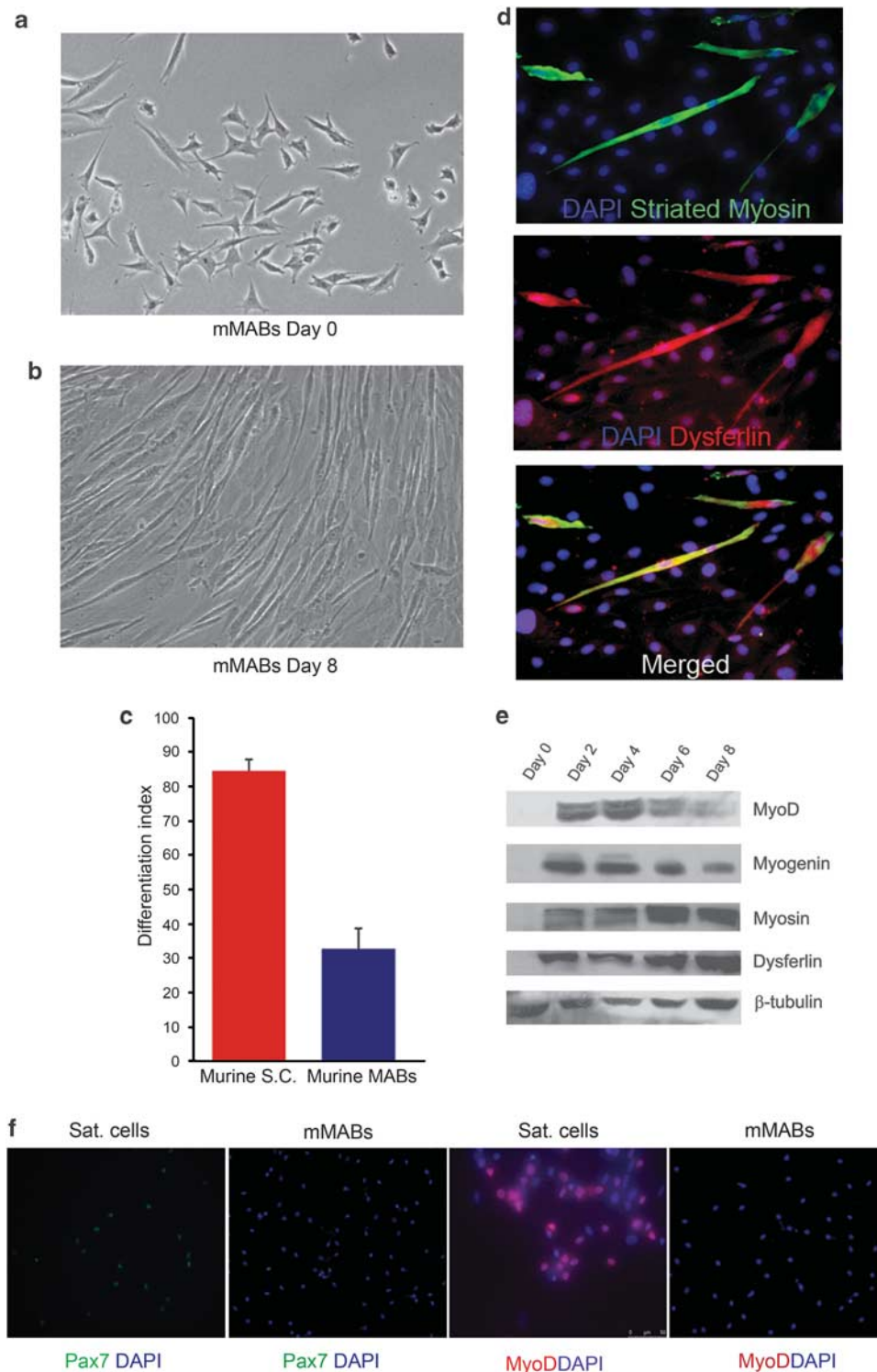


**Figure 1** Characterization of C57-J1 cells. Phase-contrast microscopy of adult-derived C57-J1 MABs revealing a small, refractile, triangular shape (a). Once confluent, cells progressively differentiated into multinucleated myotubes (b shows cells after 8 days in differentiation medium). At this stage, IF reveals that expression of striated myosin (c, top) and dysferlin (c, middle) colocalized in myotubes (c, bottom). Differentiation index, calculated as the proportion of total nuclei expressing MHC, ranged between 25 and 40% (d). Western blot analysis performed at different points during differentiation to striated muscle showing concomitant presence of MyoD, myogenin and dysferlin (e). During proliferation status C57-J1 cells did not express MyoD and Pax7 as in satellite cells (e and f)

C57-J1 cells, we trained all mice with 1 h swimming 24 h before the transplantation. We found LacZ-positive cells in all muscles situated downstream of injection site (Figure 3a and

Supplementary Figure 4). The number of LacZ-positive cells was higher in ctx-treated muscles, but LacZ fibers were clearly detected also in untreated muscles (a quantification is

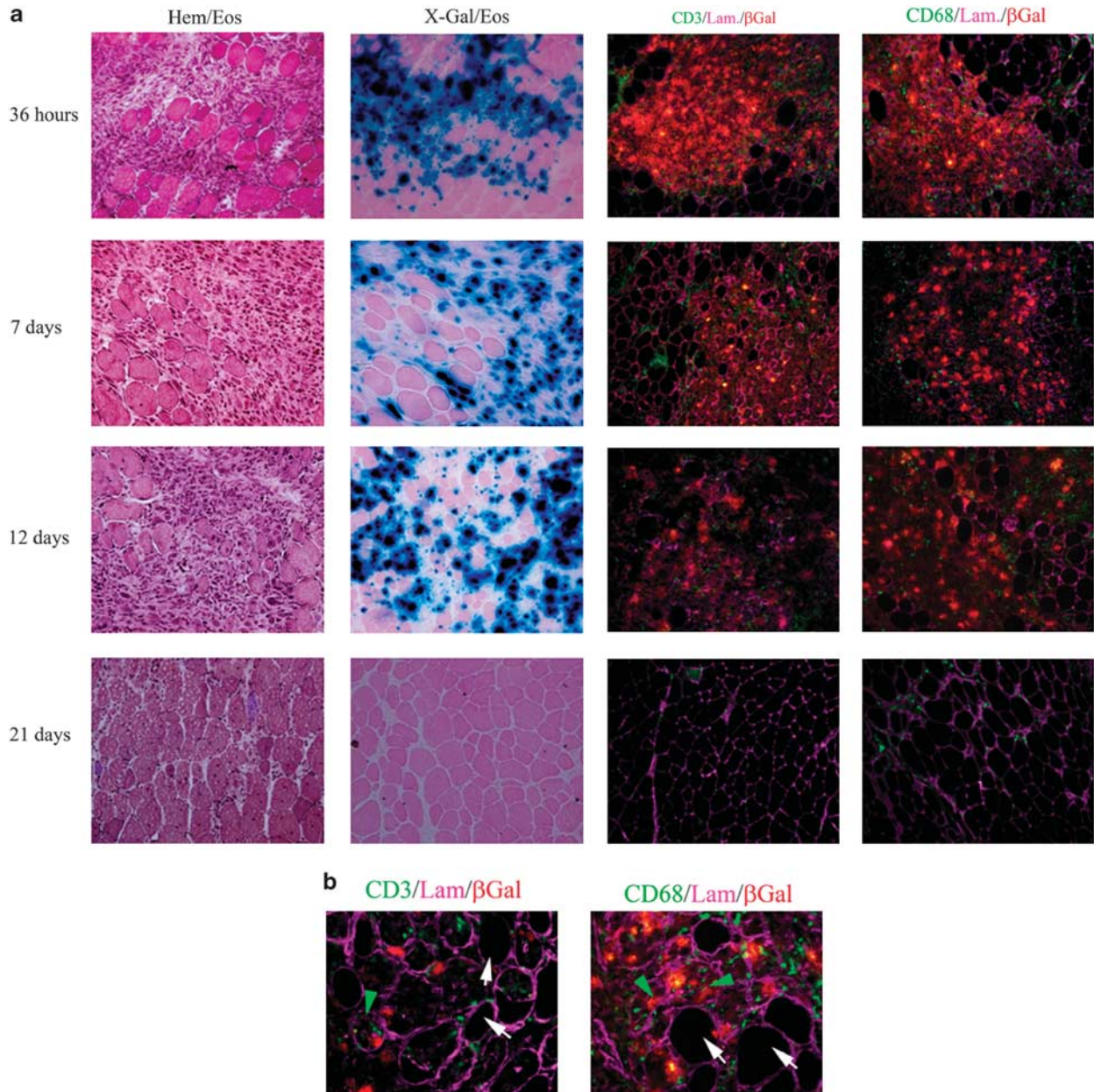


**Figure 2** Inflammatory infiltrates surrounded transplanted cells in *BIAJ* mice. Hematoxylin-eosin staining of transplanted muscles, showing intense inflammatory reaction after intramuscular injection of  $5 \times 10^5$  nLacZ-positive C57-J1 cells into tibialis anterior of 5-month-old *BIAJ* mice (a, left column). Note almost normal muscle architecture and infiltrate resolution 21 days after the injection. X-gal staining on transplanted muscles showing a progressive loss of LacZ-positive cells (a, middle left column). Immune staining with anti-CD3 and anti-CD68 antibodies detected a mixed population of T lymphocytes and macrophages composing the infiltrate (a, middle right and right column). Numerous X-gal-positive muscle fibers invaded by CD3- and CD68-positive cells were detected (b, yellow arrow) whereas X-gal negative fibers maintained its basal lamina intact (b, white arrow)

reported in Figure 3b). Real-time PCR detected statistically significant expression of dysferlin in all muscles treated using both intramuscular or intra-arterial delivery of cells (Figure 3c). When injected intramuscularly, the average level of dysferlin ranged between 17 and 27% of wild-type muscle levels in the ctx-pretreated muscles (maximum of 35% in the gastrocnemius), and between 12 and 15% in the non-ctx-treated (maximum of 28% in the tibialis anterior of one of the animals). A single intra-arterial injection of cells was sufficient

to achieve significant expression of dysferlin in all muscles analyzed. The average level in this case varied between 9 and 11% of wild-type muscles in the ctx-pretreated animals (maximum of 16% in the gastrocnemius of one animal) and between 6 and 12% in the non-ctx-treated animals (maximum of 18% in the quadriceps of one mouse). Dysferlin was detected in many fibers that invariably contained  $\beta$ -galactosidase-positive nuclei; the protein was absent in noninjected muscles (Figure 4a). Western blot (WB) analysis

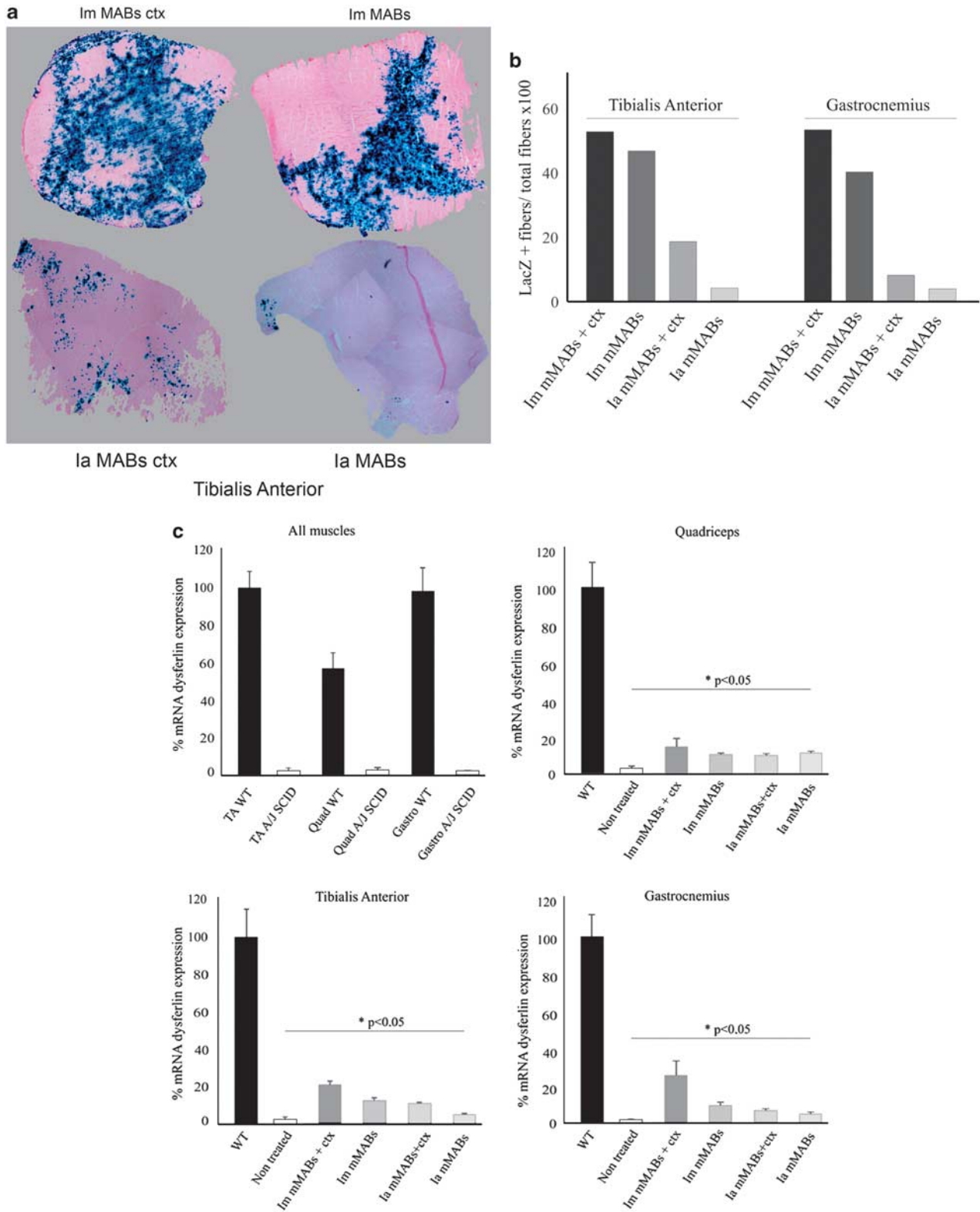


**Figure 3** C57-J1 cells successfully colonized muscles of *SCID/BLAJ* mice. X-gal staining of *SCID/BLAJ* tibialis anterior 1 month after a single intramuscular or intra-arterial injection of  $5 \times 10^5$  C57-J1 cells, previously labeled with nLacZ. At 1 month after the injection numerous LacZ-positive muscle fibers were observed (Figure 3a), localized throughout the entire area of the muscle section. Quantification of LacZ-positive fibers in tibialis anterior and gastrocnemius (Figure 3b): dysferlin mRNA was detected at significant higher levels in transplanted than in nontransplanted muscles in all conditions performed (c, tibialis anterior, quadriceps and gastrocnemius). Differences were analyzed using Student's *t*-test and considered significant if  $P < 0.05$ . Bars show mean values, with standard error. Im, intramuscular; Ia, intra-arterial; Ctx, cardiotoxin

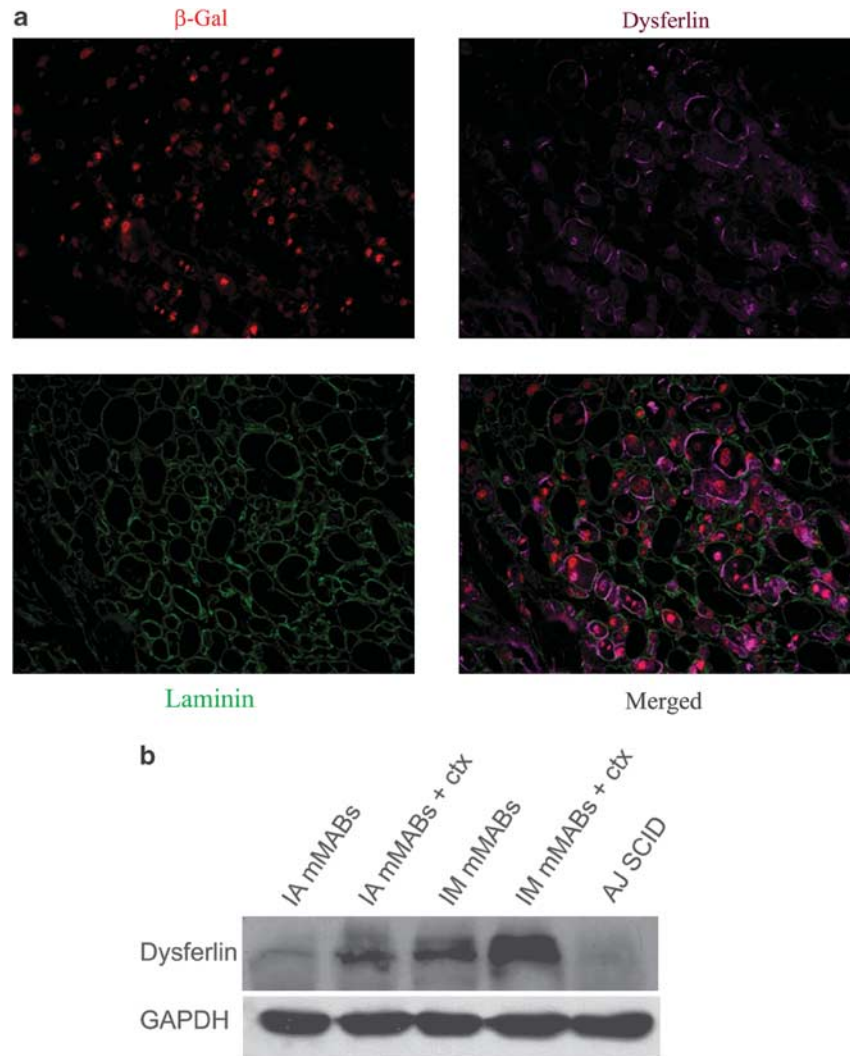


**Figure 4** Transplantation of C57-J1 cells into the *SCID/BIAJ* murine model successfully restored the expression of dysferlin. Immunofluorescence with anti-dysferlin antibodies detecting the protein only on the membrane of  $\beta$ -galactosidase-positive fibers (a). Western blot analysis of muscle lysates showing the presence of dysferlin protein in all conditions studied (b)

confirmed the findings of the real-time PCR and showed expression of the dysferlin protein in all transplanted dystrophic muscles, with a higher level in muscles previously treated with ctx (Figure 4b).

**Functional assays.** Five-month-old *SCID* mice ( $n=3$ ), control nontransplanted *SCID/BIAJ* mice ( $n=4$ ) and *SCID/BIAJ* intra-arterially transplanted with C57-J1 cells ( $n=4$ ) were tested for motor activity on the treadmill. All dystrophic untreated *SCID/BIAJ* showed worse performance in this test than control *SCID* mice but differences were not statistically significant at this age. Motility of transplanted *SCID/BIAJ* improved notably compared with untreated mice, but differences did not reach statistical significance (Supplementary Figures 5a–c). Increase in creatine kinase levels after the exercise was detected in all animals, but it was lower in the treated than in the nontreated *SCID/BIAJ* mice, without statistical significance (data not shown).

The absence of significant differences in treadmill prompted us to use another, possibly more sensitive, functional assay. As dysferlin absence causes a defect in membrane repair, we tested the ability of single fibers from transplanted mice to reseal the membrane after a focal damage produced by a laser, as previously described by Bansal *et al.*<sup>10</sup> We administered a single injection of  $5 \times 10^5$  GFP-labeled, C57-J1 cells into tibialis anterior, extensor digitorum longus and gastrocnemius of 5-month-old *SCID/BIAJ* mice. At 1 month after the injection, GFP was easily detected in all injected muscles (Figure 5a) but not in noninjected, contralateral muscles. Single fibers from control *SCID* mice ( $n=4$ ), untreated *SCID/BIAJ* ( $n=4$ ) and transplanted *SCID/BIAJ* mice ( $n=4$ ) were isolated and plated into dishes with  $\text{Ca}^{2+}$  PBS. Dysferlin was detected only in the surface of GFP-positive fibers in a patchy distribution (Figure 5b). Single fibers were irradiated with a laser in the presence of the fluorescence dye FM 4-64 to create a lesion in the plasma

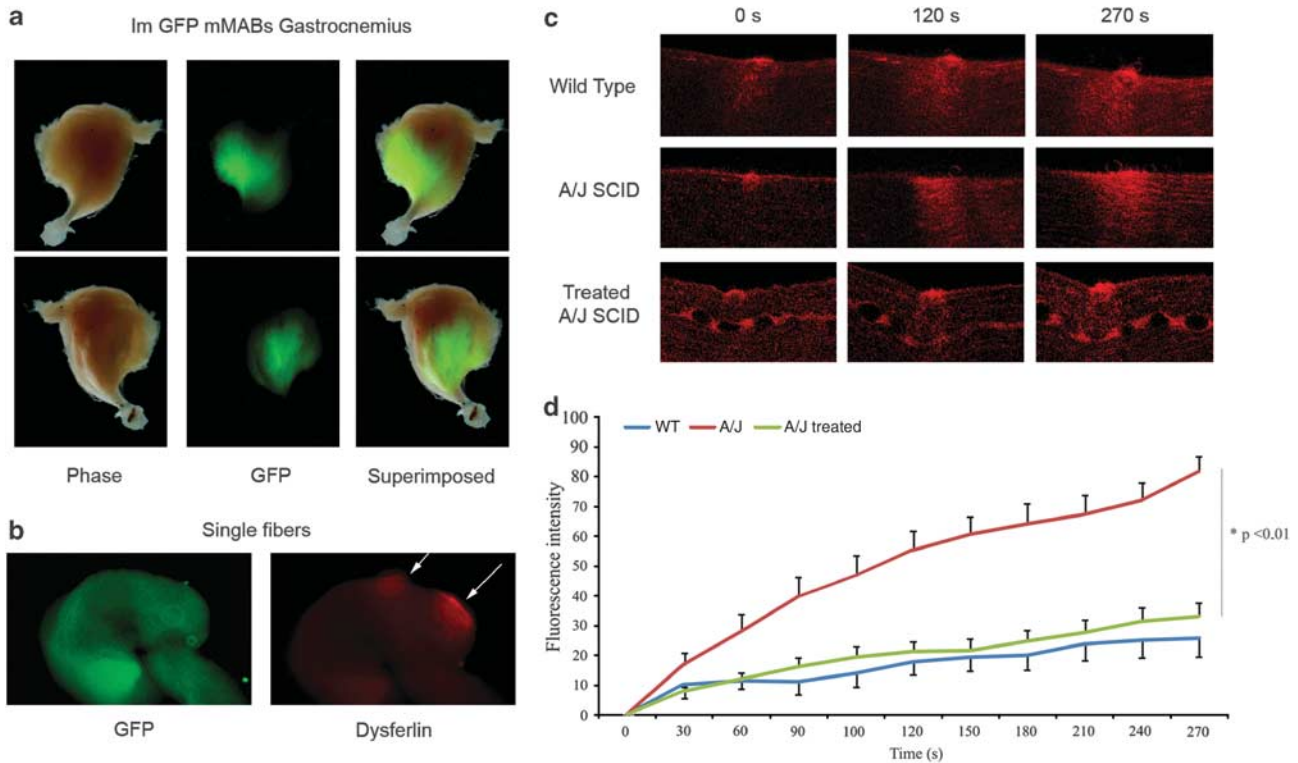


**Figure 5** Functional assays. GFP expression pattern of dystrophic tibialis anterior of 5-month-old *SCID/BLAJ* 1 month after the intramuscular injection of  $5 \times 10^5$  GFP-positive C57-J1 cells (a). Immunofluorescence analysis showing dysferlin expression on the membrane of GFP-positive single fibers in a patchy distribution (b, white arrows). Membrane repair assay was performed in isolated single fibers from WT, *SCID* (c, top panel), nontransplanted *SCID/BLAJ* (c, middle panel) and transplanted *SCID/BLAJ* (c, bottom panel) mice. Note a larger area of dye staining in the nontreated *SCID/BLAJ* fibers after laser-induced lesions (c). Measurement of fluorescence intensity versus time is shown in d for WT (blue line), nontransplanted *SCID/BLAJ* (red line) and transplanted *SCID/BLAJ* (green line) showing significant higher levels in the nontransplanted *SCID/BLAJ*. There were no differences between transplanted *SCID/BLAJ* and WT mice. Data are mean  $\pm$  S.E. (WT  $n$ :10 fibers, nontreated *SCID/BLAJ*  $n$ :15 fibers, transplanted *SCID/BLAJ*  $n$ :20 fibers); statistical analysis was carried out with Student's *t*-test and ANOVA test for repeated measurements.  $P < 0.05$  was considered significant

membrane. In this experimental model, increase in the fluorescence signal in the area adjacent to the sarcolemmal lesion inversely correlates with the resealing activity of the membrane; in fact, the increase in signal intensity rapidly stops in wild-type, dysferlin-positive fibers whereas it continues to augment in the dysferlin negative fibers.<sup>10</sup> The increase in the signal was much lower in the MABs-transplanted fibers from the *SCID/BLAJ* mice than from the nontreated mice ( $P < 0.0001$ ) and, importantly, this increase was not different from the one detected in single fibers from wild-type control mice (Figure 5c and d).

## Discussion

**New therapies for muscular dystrophies.** Muscular dystrophies still lack an efficacious therapy. In preclinical models, cell transplantation, gene therapy, exon skipping and molecules inducing muscle hypertrophy all produced encouraging results but await the results of controlled clinical experimentation.

Our laboratory pioneered progenitor cell transplantation in a murine ( $\alpha$ -sarcoglycan deficiency) and in a canine (dystrophin deficiency) model of muscular dystrophy. The success of the

transplantation depends upon a number of parameters among which the histopathology of the transplanted muscle, the presence of a resident myogenic population and the engraftment and myogenic potency of the donor cells appear the most important. For example, in the *mdx* mouse, which has vigorous endogenous regeneration, embryonic D16 MAB transplantation produced modest engraftment and dystrophin production (M Sampaolesi and G Cossu, unpublished data). It thus becomes very important to test the cell therapy protocol in other forms of muscular dystrophy, possibly using a robustly myogenic MAB population, given the fact that the D16 embryonic MABs have a modest intrinsic myogenic potency.

**Adult MABs have robust myogenic potency.** To this aim, we have isolated and characterized MABs from skeletal muscles of adult mice. Although these cells have the ability to differentiate into diverse types of mesoderm cell types, they show a robust myogenic differentiation both *in vitro* and, most importantly, when injected intramuscularly or intra-arterially in dystrophic muscle. The MABs obtained from murine adult skeletal muscle biopsies are distinguishable from SCs as they do not express CD34, MyoD or Pax7 during proliferation, although they activate MyoD when myogenesis is

induced.<sup>21</sup> Surprisingly, AP is not expressed by these cells in culture, at variance with human MABs. In murine muscles, AP is expressed *in vivo* by pericytes and by endothelial cells, but this expression is lost after serial passages in culture. Dysferlin was expressed by C57-J1 cells and also by human-derived MABs when differentiated into skeletal muscle (J Díaz-Manera and G Cossu, unpublished data).

**Adult MABs repair the dysferlinopathy in the mouse.** We showed expression of dysferlin in  $\beta$ -galactosidase-positive fibers after nLacZ-positive MAB transplantation in the *SCID/BIAJ* mice, and because revertant fibers have not been reported in the *A/J* mice, dysferlin detected by IF or WB should have been produced from transplanted cells once fused with dystrophic fibers. The *A/J* mutation results in a drastic reduction of dysferlin mRNA (<2–4% of wild-type muscle). After transplantation, dysferlin mRNA was detected in muscles at much higher levels, up to 35% of wild-type levels after a single intramuscular injection, and 18% after a single intra-arterial injection. It has been previously reported that the levels of dysferlin can be reduced in asymptomatic or mildly symptomatic carriers of the disease.<sup>22</sup> WB of muscles from heterozygous familiars of affected patients showed dysferlin expression of 40–50% compared to control levels.<sup>23</sup> Moreover, a recent analysis of the dysferlin protein levels in CD14+ monocytes from peripheral blood, which correlates with levels in skeletal muscle, showed reduced expression in 60% of asymptomatic carriers, than in some cases reached up to 80% of reduction compared to normal controls.<sup>24</sup> Thus a partial reconstitution of dysferlin, to the levels detected in this study after a single injection, should be sufficient to reduce significantly or even eliminate symptoms in affected patients.

Although myoblast transplantation had previously resulted in dysferlin expression in the tibialis anterior of SJL dystrophic mice,<sup>25</sup> no analysis of functional improvement was reported and, moreover, myoblast transplantation is limited to topic intramuscular delivery. In our study, we observed functional differences with the treadmill test, but they did not reach statistical significance likely because of the modest difference between dystrophic and control mice in this specific model. To conclusively show a functional recovery in transplanted mice, we used an assay previously described by Bansal *et al.*<sup>10</sup> that is based upon laser-induced membrane lesion. This method has recently been used to analyze response to different gene therapy strategies and is very sensitive in detecting functional recovery of dysferlin null mice treated with gene or stem cell therapy.<sup>26</sup> In our case, transplantation was followed by normal resealing activity of isolated single fibers from MAB-transplanted *SCID/BIAJ* mice, compared to the nontransplanted fibers. These results, in agreement with the reduced expression of dysferlin in asymptomatic carriers, indicate that normal levels are not necessary to obtain a complete resealing activity of the plasma membrane. Dysferlin has not a structural role in the muscle fiber as dystrophin or sarcoglycans; its activity is related to repairing of the membrane and, thus, much as it happens with proteins endowed with an enzymatic function in metabolic diseases, a partial restoration of expression would be sufficient for a virtually complete functional recovery.

The immune response obtained in the nonimmunosuppressed *BIAJ* muscles after transplantation of C57-J1 cells has been also described after myoblast transplantation in nonimmunosuppressed mice,<sup>27</sup> and might be exacerbated in this case by the expression of  $\beta$ -galactosidase by the cells and by the altered immune system of the dysferlin-deficient mice. It is known that dysferlin-deficient monocytes and macrophages show abnormally high phagocytic activity.<sup>20</sup> Moreover, the expression of DAF (or CD55), a molecule that has been related with suppression of complement activation and inhibition of the interaction of antigen-presenting cells with T lymphocytes has been shown to be reduced in dysferlin-deficient muscles.<sup>19</sup> Accordingly to this, a lower expression of DAF by grafts has been related with accelerated T-cell-mediated rejection in renal or heart transplants.<sup>28,29</sup> Therefore, a permanent immune suppression would be necessary in a hypothetical transplantation of human MABs in patients affected by this form of muscular dystrophy.

**Cell transplantation at an early stage of the disease.** To optimize therapeutic results, we decided to treat dystrophic mice in a paucisymptomatic stage, before the presence of abundant fibrous tissue or fatty infiltration of muscles. Our previous studies using MAB injection in advanced stage  $\alpha$ -sarcoglycan mice showed poor results that improved remarkably when host muscles were pretreated with cells secreting metalloproteinase-9 and placenta-derived growth factor.<sup>30</sup> We selected 5-month-old *SCID/BIAJ* because the first dystrophic changes are already recognizable, but fatty infiltration or fibrous tissue is not present yet. One of the most important characteristics of MABs is their ability to cross the vessel walls and colonize affected muscles in response to different inflammatory signals.<sup>31</sup> It has been reported that dystrophic changes in the *A/J* muscles appear quite late in life and remain confined to a minority of muscles, suggesting that few inflammatory signals should be released.<sup>7</sup> Nevertheless, C57-J1 cells were able to cross the vessel walls and massively colonize dystrophic muscles; this colonization was further enhanced by ctx-induced muscle damage and subsequent regeneration, even though this could not possibly apply to a clinical situation. Nevertheless, the higher amount of nLacZ-positive fibers in ctx-pretreated muscles suggests that inflammatory signals and chemoattractants are released at higher levels after an acute damage and consequent inflammation. Interestingly, we observed similar results with adult MABs in *mdx* dystrophic mice (G Messina, unpublished results). The ability to cross the vessel is of outstanding importance to design a therapeutic strategy in humans, as it would allow the distribution of donor cells all over the body muscles after intra-arterial injection.<sup>32</sup> Moreover, significant differences exist between skeletal muscles from dysferlinopathy human patients and *SCID/BIAJ* mice. Strong inflammatory infiltrates,<sup>33</sup> degenerating and regenerating fibers<sup>34,35</sup> are frequently recognized, especially during the first stage of the disease in humans, when some cases has been misdiagnosed as inflammatory myopathies.<sup>36</sup> This inflammatory activity would hypothetically enhance the migration of MABs from the vessel to muscles in patients but an equilibrium should be found to prevent an



exacerbated tissue reaction against donor cells even in the presence of immune suppression.

In conclusion, we have shown that adult murine MABs, when transplanted into the *SCID/BLAJ* mice, partially restored the expression of dysferlin to levels that allowed a normal membrane resealing activity of single fibers. These results may lead to the first therapeutic assays in patients affected by muscular dystrophies secondary to dysferlin deficiency.

## Materials and Methods

**Isolation of MABs from mouse muscular biopsies.** Murine MABs were isolated from a 2-month-old *C57BL/6* female as previously described.<sup>17</sup> Briefly, both tibialis anterior were dissected and minced in 1–2 mm pieces. Fragments were selected, transferred onto collagen type I (Sigma, St. Louis, MO, USA) coated dishes and incubated in PM consisting of Dulbecco's modified Eagle's medium (DMEM) (Sigma) supplemented with 20% fetal bovine serum (Lonza, Verviers, Belgium), 2 mM L-glutamine (Sigma), 1 mM sodium pyruvate (Sigma), 100 IU ml<sup>-1</sup> penicillin and 100 mg ml<sup>-1</sup> streptomycin (Sigma), at 37°C, 5% CO<sub>2</sub> and 5% O<sub>2</sub>. After 5–7 days, the mixed cell population deriving from primary culture outgrowth was enzymatically dissociated by collagenase/dispase treatment. Cells obtained by dissociation were counted by Trypan blue exclusion, using a hemocytometer, and immediately used for cloning. The cell suspension was cloned in PM by limiting dilution in 96-multiwell dishes and incubated at 37°C, 5% CO<sub>2</sub> and 5% O<sub>2</sub>. After 7–10 days first clones of cells were distinguishable. Once the cells covered almost 50% of the well surface, the clones were passed and propagated in PM. The majority of clones adopted after a few passages a large, flat morphology and underwent proliferative senescence. A few clones however maintained a small, refractile, poorly adhering morphology and continued to proliferate for at least 40 passages. One of these clones, C57-J1 has been used for the experiments here described.

**In vitro differentiation assay.** Spontaneous skeletal myogenic differentiation of C57-J1 cells was induced by plating 75 × 10<sup>3</sup> cells onto reduced growth factor Matrigel-coated dishes (Becton Dickinson Biosciences, San Jose, CA, USA). Differentiation medium consisted of DMEM supplemented with 2% horse serum (Sigma), 2 mM L-glutamine, 1 mM sodium pyruvate and 100 IU ml<sup>-1</sup> penicillin and 100 mg ml<sup>-1</sup> streptomycin. Cultures were incubated at 37°C, 5% CO<sub>2</sub> for different periods and then processed for IF and WB analysis. The differentiation index was calculated as the ratio between nuclei expressing myosin heavy chain (MHC) and the total number of nuclei.

Differentiation in smooth muscle cells and osteoblasts was induced by treatment with TGF-β (Sigma) and BMP-2 (PeproTech, Rocky Hill, NJ, USA) respectively, and analyzed as previously described.<sup>21</sup> To induce differentiation in adipose cells, we grew MABs in adipogenic-inducing medium (Lonza) for approximately 5 days, as described previously.<sup>17</sup>

**Flow cytometry.** C57-J1 cells in culture were analyzed by flow cytometry as previously reported.<sup>16</sup> The antibodies used for this analysis were the following: anti-CD-44 FITC, anti-CD-34 FITC, anti-CD-45 PE, anti-CD 117-PE, anti-Flk-1-PE, anti-Sca-1-PE (all from Becton Dickinson Biosciences) and anti-CD 31 FITC (ID Laboratories, London, Canada).

**Satellite cell cultures.** SCs were isolated from skeletal muscles of 10-day-old *C57BL/6* pups. Muscle fragments were mechanically minced until a fine mixture was obtained. This mixture was then digested with collagenase (Sigma) and dispase (Gibco, Paisley, UK) for 20 min at 37°C with gentle agitation. After the incubation, isolated cells were collected and fragments were incubated again until the whole tissue was digested (usually three times). Isolated cells were pooled, centrifuged and resuspended in DMEM supplemented with 20% fetal bovine serum, 2 mM L-glutamine, 1 mM sodium pyruvate, 100 IU ml<sup>-1</sup> penicillin, 100 mg ml<sup>-1</sup> streptomycin, 3% chicken embryo extract, 1% gentamicin and 50 nM basic FGF (PeproTech). Contamination by nonmyogenic cell was reduced by preplating the cell suspension onto plastic dishes where fibroblasts tend to adhere more rapidly. Differentiation was induced shifting the medium to DMEM supplemented with 5% horse serum.

**Generation of *scid/BLAJ* mice.** *BLAJ* mice (gift from I Richard, Généthon) were bred onto the *scid/scid* (severe combined immune deficient) strain, homozygous for the mutation located on chromosome 16. Resulting F1 heterozygous siblings were intercrossed to obtain homozygotes for both loci: *dysf* and *scid*.

**Cell transduction with lentiviral vectors.** Cells were transduced, as previously described,<sup>14</sup> with third-generation lentiviral vectors expressing nLacZ.

**Intramuscular delivery of MABs.** All animal studies presented in this paper were approved by the San Raffaele Institutional Review Board. Five-month-old *BLAJ* ( $n = 7$ ) and *SCID/BLAJ* ( $n = 6$ ) mice were used for intramuscular injection of cells. When used, ctx was injected into both tibialis anterior, gastrocnemius (25 μl, 100 μM) and quadriceps (50 μl, 100 μM), 24 h before the transplantation of cells. Previous to the transplantation, mice were anesthetized with an intraperitoneal injection of Avertin, containing *tert*-amyl Alcohol (2.5 ml; Sigma) and 2,2,2-tribromoethanol (2.5 g; Sigma) in 100 ml 0.9% saline serum. Intramuscular delivery was performed by injection of approximately 5 × 10<sup>5</sup> C57-J1 cells, previously transduced with lentiviral vector expressing nLacZ, into tibialis anterior, gastrocnemius and quadriceps using a 30 gauge needle. Animals were killed 1 month after the transplantation, muscles were collected and the expression of dysferlin was analyzed by IF, real-time PCR and WB.

**Intra-arterial delivery of MABs.** Five-month-old *SCID/BLAJ* mice ( $n = 10$ ) were used for the intra-arterial delivery of the cells. All mice were trained by 1 h swimming 24 h before the transplantation. When used, ctx was injected into both tibialis anterior, gastrocnemius (25 μl, 100 μM) and quadriceps (50 μl, 100 μM), just after the exercise. Previous to the transplantation, mice were anesthetized with Avertin (see receipt above). For intra-arterial delivery, approximately 5 × 10<sup>5</sup> nLacZ C57-J1 cells were injected into the right femoral artery. A limited incision on the medial upper side of the leg was performed; femoral artery was identified and carefully isolated from femoral nerve and vein. Cells were injected by a 30 gauge needle inserted into the artery. After injection, body wall muscles and skin were closed with sutures. Animals were killed 1 month after the injection, muscles were collected and the expression of dysferlin was analyzed by IF, real-time PCR and WB.

**Immunoblotting.** WB analysis of cells and tissues was performed as described.<sup>18</sup> Antibodies used were mouse anti-dysferlin Hamlet (Novacastra, Newcastle upon Tyne, UK) at 1 : 100 dilution, mouse anti-MyoD (Dako, Carpinteria, CA, USA) at 1 : 100 dilution, mouse anti-myogenin (Hybridoma Bank, Iowa City, IA, USA) at 1 : 2 dilution, mouse anti-MHC (Hybridoma Bank) at 1 : 2 dilution, mouse anti-GAPDH at 1 : 5000 (Sigma) and mouse anti-β-tubulin (Covance, Princeton, NJ, USA) at 1 : 5000 dilution.

**Immunofluorescence.** Cell cultures were washed three times with PBS and fixed with 4% paraformaldehyde at 4°C for 10 min. Muscle samples were frozen in liquid nitrogen cooled isopentane and serial 8-mm-thick sections were cut with a Leica cryostat (Leica Microsystems GmbH, Wetzlar, Germany). Cells and tissue sections were processed for IF microscopy as previously described.<sup>12</sup> The antibodies used were mouse anti-dysferlin Hamlet (Novacastra) at 1 : 20 dilution, rabbit anti-dysferlin (GenWay, San Diego, CA, USA) at 1 : 50 dilution, mouse anti-MHC (Hybridoma Bank) at 1 : 2 dilution, mouse anti-Pax 7 (Hybridoma Bank) at 1 : 2 dilution, mouse anti-MyoD (Dako) at 1 : 100 dilution, rabbit anti-GFP (Chemicon International, Temecula, CA, USA) at 1 : 300 dilution, rabbit anti-laminin (Sigma) at 1 : 300 dilution, goat anti-β-galactosidase (Biogenesis, Poole, UK) at 1 : 300, rat anti-CD68 (AbD Serotec, Raleigh, NC, USA) at 1 : 100 and rat anti-CD3 (Santa Cruz Biotechnology, Santa Cruz, CA, USA) at 1 : 100. The staining for X-Gal was performed as previously described.<sup>37</sup>

**Real-time PCR.** Total RNA from muscles was isolated using TRIzol protocol (Invitrogen, Carlsbad, CA, USA). RNA (1 μg) was reverse transcribed into cDNA using the cDNA synthesis ThermoScript RT-PCR System kit (Invitrogen). Primers used for amplify cDNA were the following: dysferlin primer: forward 5'-TCC GAAGCTAGA GGATCAA-3'; reverse 5'-AGCTTCAATGCGAGCGTAGTT-3' and murine cyclophilin: forward 5'-CATACGGTCCCTGGCATCTTGTC-3'; reverse 5'-TGGTGATCTTCTGCTGGTCTTGC-3'. Each cDNA sample was amplified in triplicate using the SYBR Green supermix (Invitrogen). Student's *t*-test was used

to analyze the differences between muscles and conditions of treatment, setting  $P < 0.05$  as significant.

**Exercise protocols.** Control 6-month-old *SCID* mice ( $n = 3$ ), nontransplanted *SCID/BLA/J* mice ( $n = 4$ ) and *SCID/BLA/J* mice transplanted with C57-J1 cells by intra-arterial injection ( $n = 4$ ) were tested for functional recovery with the treadmill test (Columbus Instruments, Columbus, OH, USA). Transplanted mice were tested at 21 days after the injection. Mice were adapted to the procedure (10 min every other day; 3 m/min at 0° inclination) for 1 week before beginning the exercise training protocol. For the exercise test, mice were put into a 10° inclined treadmill at 10 m/min, then the speed was increased by 2 m/min every 2 min until the mouse reached exhaustion, which was defined as a prolonged spending time (10 s) on the shocker plate without attempting to reengage the treadmill, or when a fixed speed of 46 m/min was reached. Total distance, running time and work was registered for every mouse. Work was calculated as the body weight (kg), gravity (9.81 m/s<sup>2</sup>), vertical speed (m/s × angle) and time (s).

Creatine kinase blood levels were analyzed 5 days before the exercise test and 6 h after the exercise following manufacturer's instruction (CK-MB detection kit; Randox Laboratories, Crumlin, UK).

**Membrane repair assay on skeletal muscle single fibers.** Control dysferlin-positive *SCID* mice ( $n = 4$ ), dystrophic, nontransplanted *SCID/BLA/J* ( $n = 4$ ) mice and transplanted *SCID/BLA/J* mice ( $n = 4$ ) were used for this experiment. *SCID/BLA/J* mice were used 1 month after the intramuscular injection of GFP-labeled C57-J1 cells. Single fibers were extracted from gastrocnemius, extensor digitorum longus and tibialis anterior as previously described.<sup>38</sup> Fibers were washed, resuspended in Dulbecco's PBS containing 1 mM Ca<sup>2+</sup> (Invitrogen, Eugene, OR, USA) and mounted on glass bottom culture dishes (MatTek, Ashland, MA, USA) in the presence of 10 μm of the fluorescent dye FM 4-64 (Invitrogen). To induce the damage, we irradiated a 7 × 7 μm area of the membrane of muscle fibers with the lasers 488 at 50% of power and 405 at 100% AOTF for 45 s. Images were captured every 30 s for 6 min after the irradiation. For every image taken, the fluorescence intensity variation at the site of the damage was measured with the ImageJ imaging software (National Institute of Health, Bethesda, MD, USA; <http://rsbweb.nih.gov/ij/index.html>). ANOVA test for repeated measurements and Student's *t*-test for every time acquisition were used to identify significant differences in the increase of light intensity.  $P < 0.05$  was considered to be significant.

### Conflict of Interest

The authors declare no conflict of interest.

**Acknowledgements.** This work was supported by a Scientific Fellowship from the European Federation of Neurological Societies, a grant from the Spanish Ministry of Health (BAE) and the special collaboration of Fundación Isabel Gemio to JDM, and by grants from Telethon, AFM, Duchenne Parent Project, EC (Optistem, Angioscaff), ERC and the Italian Ministry of Research and Health to GC. We thank D Covarello for technical assistance; C Covino for support with the confocal microscope; P Pessina, S Brunelli, E Gallardo and N De Luna for critical comments on the paper and I Richard for the *BLA/J* mice.

- Liu J, Aoki M, Illa I, Wu C, Fardeau M, Angelini C et al. Dysferlin, a novel skeletal muscle gene, is mutated in Miyoshi myopathy and limb girdle muscular dystrophy. *Nat Genet* (1998); **20**: 31–36.
- Illia I, Serrano-Munuera C, Gallardo E, Lasa A, Rojas-Garcia R, Palmer J et al. Distal anterior compartment myopathy: a dysferlin mutation causing a new muscular dystrophy phenotype. *Ann Neurol* (2001); **49**: 130–134.
- Paradas C, Gonzalez-Quereda L, De Luna N, Gallardo E, Garcia-Consuegra I, Gomez H et al. A new phenotype of dysferlinopathy with congenital onset. *Neuromuscul Disord* (2009); **19**: 21–25.
- Bushby KM. Making sense of the limb-girdle muscular dystrophies. *Brain* (1999); **122** (Pt 8): 1403–1420.
- Zatz M, de Paula F, Starling A, Vainzof M. The 10 autosomal recessive limb-girdle muscular dystrophies. *Neuromuscul Disord* (2003); **13**: 532–544.
- Ho M, Post CM, Donahue LR, Lidov HG, Bronson RT, Goolsby H et al. Disruption of muscle membrane and phenotype divergence in two novel mouse models of dysferlin deficiency. *Hum Mol Genet* (2004); **13**: 1999–2010.
- Kobayashi K, Izawa T, Kuwamura M, Yamate J. The distribution and characterization of skeletal muscle lesions in dysferlin-deficient SJL and A/J mice. *Exp Toxicol Pathol* 2009, in press.
- Bansal D, Campbell KP. Dysferlin and the plasma membrane repair in muscular dystrophy. *Trends Cell Biol* (2004); **14**: 206–213.
- Selcen D, Stilling G, Engel AG. The earliest pathologic alterations in dysferlinopathy. *Neurology* (2001); **56**: 1472–1481.
- Bansal D, Miyake K, Vogel SS, Groh S, Chen CC, Williamson R et al. Defective membrane repair in dysferlin-deficient muscular dystrophy. *Nature* (2003); **423**: 168–172.
- Cai C, Weisleder N, Ko JK, Komazaki S, Sunada Y, Nishi M et al. Membrane repair defects in muscular dystrophy are linked to altered interaction between MG53, caveolin-3, and dysferlin. *J Biol Chem* (2009); **284**: 15894–15902.
- Minasi MG, Riminucci M, De Angelis L, Borello U, Berarducci B, Innocenzi A et al. The meso-angioblast: a multipotent, self-renewing cell that originates from the dorsal aorta and differentiates into most mesodermal tissues. *Development* (2002); **129**: 2773–2783.
- Cossu G, Sampaolesi M. New therapies for Duchenne muscular dystrophy: challenges, prospects and clinical trials. *Trends Mol Med* (2007); **13**: 520–526.
- Sampaolesi M, Torrente Y, Innocenzi A, Tonlorenzi R, D'Antona G, Pellegrino MA et al. Cell therapy of alpha-sarcoglycan null dystrophic mice through intra-arterial delivery of mesoangioblasts. *Science* (2003); **301**: 487–492.
- Sampaolesi M, Blot S, D'Antona G, Granger N, Tonlorenzi R, Innocenzi A et al. Mesoangioblast stem cells ameliorate muscle function in dystrophic dogs. *Nature* (2006); **444**: 574–579.
- Dellavalle A, Sampaolesi M, Tonlorenzi R, Tagliafico E, Sacchetti B, Perani L et al. Pericytes of human skeletal muscle are myogenic precursors distinct from satellite cells. *Nat Cell Biol* (2007); **9**: 255–267.
- Tonlorenzi R, Dellavalle A, Schnapp E, Cossu G, Sampaolesi M. Isolation and characterization of mesoangioblasts from mouse, dog, and human tissues. *Curr Protoc Stem Cell Biol* 2007; (Supp 3), Chapter 2: Unit 2B 1.
- Messina G, Blasi C, La Rocca SA, Pompili M, Calconi A, Grossi M. p27Kip1 acts downstream of N-cadherin-mediated cell adhesion to promote myogenesis beyond cell cycle regulation. *Mol Biol Cell* (2005); **16**: 1469–1480.
- Wenzel K, Zabojszcza J, Carl M, Taubert S, Lass A, Harris CL et al. Increased susceptibility to complement attack due to down-regulation of decay-accelerating factor/CD55 in dysferlin-deficient muscular dystrophy. *J Immunol* (2005); **175**: 6219–6225.
- Nagaraju K, Rawat R, Veszelszky E, Thapliyal R, Kesari A, Sparks S et al. Dysferlin deficiency enhances monocyte phagocytosis: a model for the inflammatory onset of limb-girdle muscular dystrophy 2B. *Am J Pathol* (2008); **172**: 774–785.
- Messina G, Sirabella D, Monteverde S, Galvez BG, Tonlorenzi R, Schnapp E et al. Skeletal muscle differentiation of embryonic mesoangioblasts requires pax3 activity. *Stem Cells* (2009); **27**: 157–164.
- Illia I, De Luna N, Dominguez-Perles R, Rojas-Garcia R, Paradas C, Palmer J et al. Symptomatic dysferlin gene mutation carriers: characterization of two cases. *Neurology* (2007); **68**: 1284–1289.
- Fanin M, Nascimbeni AC, Angelini C. Muscle protein analysis in the detection of heterozygotes for recessive limb girdle muscular dystrophy type 2B and 2E. *Neuromuscul Disord* (2006); **16**: 792–799.
- De Luna N, Gallardo E, Rojas-Garcia R, Dominguez-Perles R, Díaz-Manera J, De La Torre C et al. Quantification of dysferlin in monocytes: a useful tool for the detection of patients and carriers of dysferlinopathy. *Neuromuscul Disord* (2009); **18**: 790–791.
- Leriche-Guerin K, Anderson LV, Wrogemann K, Roy B, Goulet M, Tremblay JP. Dysferlin expression after normal myoblast transplantation in SCID and in SJL mice. *Neuromuscul Disord* (2002); **12**: 167–173.
- Lostal W, Bartoli M, Bourg N, Roudaut C, Bentaib A, Miyake K et al. Efficient recovery of dysferlin deficiency by dual adeno-associated vector-mediated gene transfer. *Hum Mol Genet* (2010); **19**: 1897–1907.
- Skuk D, Tremblay JP. Progress in myoblast transplantation: a potential treatment of dystrophies. *Microsc Res Tech* (2000); **48**: 213–222.
- Pavlov V, Raedler H, Yuan S, Leisman S, Kwan WH, Lalli PN et al. Donor deficiency of decay-accelerating factor accelerates murine T cell-mediated cardiac allograft rejection. *J Immunol* (2008); **181**: 4580–4589.
- Brodsky SV, Nadasdy GM, Pelletier R, Satoskar A, Birmingham DJ, Hadley GA et al. Expression of the decay-accelerating factor (CD55) in renal transplants – a possible prediction marker of allograft survival. *Transplantation* (2009); **88**: 457–464.
- Gargioli C, Coletta M, De Grandis F, Cannata SM, Cossu G. PlGF-MMP-9-expressing cells restore microcirculation and efficacy of cell therapy in aged dystrophic muscle. *Nat Med* (2008); **14**: 973–978.
- Palumbo R, Sampaolesi M, De Marchis F, Tonlorenzi R, Colombetti S, Mondino A et al. Extracellular HMGB1, a signal of tissue damage, induces mesoangioblast migration and proliferation. *J Cell Biol* (2004); **164**: 441–449.
- Peault B, Rudnicki M, Torrente Y, Cossu G, Tremblay JP, Partridge T et al. Stem and progenitor cells in skeletal muscle development, maintenance, and therapy. *Mol Ther* (2007); **15**: 867–877.

33. Gallardo E, Rojas-Garcia R, de Luna N, Pou A, Brown Jr RH, Illa I. Inflammation in dysferlin myopathy: immunohistochemical characterization of 13 patients. *Neurology* (2001); **57**: 2136–2138.
34. Fanin M, Angelini C. Muscle pathology in dysferlin deficiency. *Neuropathol Appl Neurobiol* (2002); **28**: 461–470.
35. Linssen WH, Notermans NC, Van der Graaf Y, Wokke JH, Van Doorn PA, Howeler CJ *et al*. Miyoshi-type distal muscular dystrophy. Clinical spectrum in 24 Dutch patients. *Brain* (1997); **120** (Pt 11): 1989–1996.
36. Nguyen K, Bassez G, Krahn M, Bernard R, Laforet P, Labelle V *et al*. Phenotypic study in 40 patients with dysferlin gene mutations: high frequency of atypical phenotypes. *Arch Neurol* (2007); **64**: 1176–1182.
37. Tajbakhsh S, Vivarelli E, Cusella-De Angelis G, Rocancourt D, Buckingham M, Cossu G. A population of myogenic cells derived from the mouse neural tube. *Neuron* (1994); **13**: 813–821.
38. Rosenblatt JD, Lunt AI, Parry DJ, Partridge TA. Culturing satellite cells from living single muscle fiber explants. *In Vitro Cell Dev Biol Anim* (1995); **31**: 773–779.



**Cell Death and Disease** is an open-access journal published by *Nature Publishing Group*. This work is licensed under the **Creative Commons Attribution-NonCommercial-No Derivative Works 3.0 Unported License**. To view a copy of this license, visit <http://creativecommons.org/licenses/by-nc-nd/3.0/>

Supplementary Information accompanies the paper on Cell Death and Disease website (<http://www.nature.com/cddis>)